Survey of Pediatric Fluoroscopic Air Kerma Rate Values and Recommended Application of Results

**The Report of AAPM
Task Group 251**

April 2022

This page intentionally left blank.

Corrigenda

Errata sheet listing chronologically the changes in the report. Please, check it often to verify that you have an updated version of the report.

Date	Change	Comments
August 7 2022	Replaced Figure 5 with the correct figure	The report as first published printed Figure 7 twice, once where it belonged and once where Figure 5 should have been.

Survey of Pediatric Fluoroscopic Air Kerma Rate Values and Recommended Application of Results

The Report of AAPM Task Group 251

Usman Mahmood[1], Chair; Lawrence T. Dauer[1]; Ishtiaq H. Bercha[2]; Samuel L. Brady[3];

Thomas M. Cummings[4]; Cristina T. Dodge[5]; David W. Jordan[6]; Nima Kasraie[7];

Mary A. Keenan[8]; Mohammed H. Aljallad[9]; Don-Soo Kim[10]; Andrew T. Kuhls-Gilcrist[11];

Sarah E. McKenney[12]; Richard Miguel[13]; Donald L. Miller[14]; Vikas Patel[15];

David Spellic[14]; Charles E. Willis[16]; Xiaowei Zhu[17]; and Keith J. Strauss[3]

Consultant: Laurel Burke[14]

[1]Memorial Sloan Kettering Cancer Center, New York, NY
[2]Yale New Haven Hospital, New Haven, CT
[3]Children's Hospital Medical Center, Cincinnati, OH
[4]NYU Langone Medical Center, New York, NY
[5]Texas Children's Hospital, Houston, TX
[6]University Hospitals Cleveland Medical Center, Cleveland, OH
[7]UT Southwestern Medical Center, Dallas, TX
[8]Vanderbilt University Medical Center, Nashville, TN
[9]Children's Mercy Hospitals and Clinics, Kansas City, MO
[10]Boston Children's Hospital, Boston, MA
[11]Canon Medical Systems, Tustin, CA
[12]Stanford University, Stanford, CA
[13]West Physics, Atlanta, GA
[14]Center for Devices and Radiological Health, Food and Drug Administration, Silver Spring, MD
[15]Upstate Medical Physics, Victor, NY
[16]MD Anderson Cancer Center, Houston, TX
[17]The Children's Hospital of Philadelphia, Philadelphia, PA

Contents

1. Introduction

The AAPM charged Task Group 251 (TG-251) with collecting fluoroscopic and fluorographic air kerma rates (AKRs) as a function of simulated patient thickness from infants to adult-sized patients, to survey the state of the practice, and to disseminate this information so that qualified medical physicists (QMPs) could compare their measurements for a typical range of patient sizes to the task group's published results.

An increase in novel interventional applications has accompanied advances in fluoroscopic hardware and software, but the rate of advancement has outpaced educational initiatives on how best to integrate new technologies (Balter 2006). Consequently, fluoroscopic equipment sold to hospitals may, at times, be used in clinical practice with the default manufacturer settings and no additional configurational changes to adapt further image quality and radiation dose for a diagnostic task or the patient population specific to that institution (Strauss 2015c). Systems using default settings (i.e., not configured for the pediatric population) may deposit excessive radiation dose or require repeat exams due to suboptimal image quality (Strauss 2006a & b). In such settings, pediatric populations are of concern, especially given that 70% of pediatric hospitalizations occur at general hospitals (Leyenaar 2016).

Both stochastic and deterministic risks are associated with substantial doses of ionizing radiation. Effective radiation doses per examination of more than 100 mSv (AAPM 2018) are believed to be the lower threshold for stochastic risks, while the lower threshold for a deterministic skin injury is a peak skin dose of 2000 mGy (NCRP 2012). Stochastic radiation risks are typically a greater concern for pediatric patients than adults, both because of the long-expected survival of children and their higher overall sensitivity to some stochastic effects (Strauss 2006a & b; Ferro 2015; Damilakis 2019). An earlier generalization that children might be three to five times more sensitive to radiation than adults (Hall 2006) may not be accurate for all stochastic effects. The United Nations Scientific Committee on the Effects of Atomic Radiation (UNSCEAR 2013) noted that children might be more radiosensitive than adults for leukemia, thyroid, skin, breast, and brain cancer. However, in many cases, the data are too weak to conclude differences in risk with age at exposure. For small, younger pediatric patients, deterministic radiation risks may be less of a concern than stochastic risks because the peak skin dose threshold of 2000 mGy is not reached, except possibly for complex interventional fluoroscopic procedures.

According to UNSCEAR (2013), similar complex radiosensitivity comparisons between children and adults are seen for deterministic tissue reactions. Due to their larger size, the peak skin dose for large adults may be an order of magnitude more than for a small pediatric patient for the same interventional fluoroscopic examination, making deterministic skin effects more likely for the adult patient. However, since the middle-aged adult typically has a shorter remaining lifetime than the pediatric patient, the likelihood of cancer with a 25- to 30-year latent period being expressed is smaller for the adult patient than for a pediatric patient.

Nevertheless, the radiation dose delivered to pediatric patients should be carefully managed to minimize stochastic and deterministic effects while also accounting for effects on image quality (Strauss 2006a & b; Lederman 2002). These effects depend upon the technology used, examination type, settings applied, disease-related factors, and the child's anatomical and physiological characteristics. Relative to most adults, children have smaller body parts, less overlying tissue to shield critical organs during radiation exposures, and lack the fat planes between organs that could enhance contrast and tissue differentiation (MITA 2015). Consequently, for a fixed air kerma rate at the entrance plane of the patient, the dose to any organ in a pediatric patient will be higher than for an adult patient (UNSCEAR 2013). Although small body habitus will cause properly calibrated fluoroscopic equipment to reduce the dose rate (Kaye 2000; Aria 2014), the increased complexity in imaging and diffi-

culty in gaining access into small regions of anatomy may result in longer fluoroscopy times, higher frame rates, or more use of fluorographic modes (NCRP 2012).

Outreach efforts by organizations such as Image Gently (Sidhu 2009; Strauss 2015b; IGA 2014a–d) have emphasized that experienced pediatric interventional operators should perform pediatric interventional procedures using appropriately configured fluoroscopes, but several recent studies have shown that many medical centers lack specialized pediatric care and equipment (CPEM 2007; Sullivan 2013; Franca 2018; Ray 2018).

Given the increasing frequency, complexity, and length of fluoroscopy-guided interventional (FGI) procedures (ICRP 2013), it is important to mitigate risks in pediatric patients by configuring fluoroscopic equipment appropriately for the clinical task. However, fluoroscopes configured to image the limited range of adult patient sizes may not adequately manage the incident air kerma rates (AKRs) to small children, e.g., 4–10 kg. In response to this task group's AAPM charge (stated following the table of contents of this report), the task group developed a standardized protocol to measure state-of-the-practice AKR values as a function of patient thickness from different types of fluoroscopes employed in both pediatric and adult medical centers, both academic and non-academic.

While maintaining diagnostic image quality and proper management of AKRs during fluoroscopic examinations are equally important, the AAPM charge did not include evaluation of image quality. Protocols should have been established with assistance from the vendor application specialists in collaboration with clinicians and the qualified medical physicist (QMP) if available at the time of installation. Poor image quality should have led to assessing and adjusting equipment settings until they were appropriate for the clinical task. In some cases, it may be necessary to increase AKRs to ensure that image quality is sufficient for the clinical task. On the other hand, fluoroscopy systems with excessive AKRs may produce high-quality images with little to no noise. As a result, the higher radiation dose rates will likely remain unless identified by the QMP during annual performance testing of the equipment. This, however, will only happen if the QMP's assessment of AKR includes measurements for simulated thicknesses of pediatric patients and has information on AKRs for pediatric patients relative to adult-sized patient AKRs for the unit being tested (Miller 2010).

The charge of the AAPM also did not include the development of diagnostic reference levels (DRLs) that pertain to the cumulative AK of the fluoroscopic examination. They are determined by the performance of the fluoroscope and operator. Readers are referred to various sources (ICRP 2007; NCRP 2010; EC 2014; Strauss 2015a; Strauss 2015c; Ubeda 2015; ICRP 2017; Kottou 2018) for a discussion of the role of DRLs in fluoroscopic imaging.

2. Methods

AAPM Report 11 (TG-11) (Boone et al. 1993) measured AKRs for pre-defined, adult-oriented protocols on various fluoroscopic equipment. In addition, the RAD-IR study (Balter 2004-Part III) developed a comprehensive measurement protocol using varying thicknesses of polymethylmethacrylate (PMMA), where the range of PMMA thicknesses represented patient sizes generally seen among adults. Similar to these two studies, TG-251 was tasked with establishing a measurement protocol that would allow for reproducibility and practicality. TG-251 adopted an approach similar to TG-11 to develop a standardized pediatric-focused protocol where variable thicknesses of PMMA—small enough to simulate infant extremity and trunk attenuation up to adult-sized patients—were used to measure AKR from fluoroscopes. For each surveyed fluoroscopic unit, AKR was measured for the fluoroscopic and fluorographic modes. When displayed by the fluoroscope, the pulse width, tube potential (kV), and root mean squared tube current (RMS mA) were recorded for both fluoroscopic and fluorographic configurations. In some cases, when pulse width was not displayed, the full width at half maximum (FWHM) of a pulse of tube potential waveform was measured.

Table 1: Vendors Included in This TG by Equipment Type

Distribution by Equipment Type					
Manufacturer	Mini C-Arms	Mobile C-Arms	General Fluoro (GF)	IRR[1] or IRC[2]	Cardiac EP[3]
Phillips	–	3 (8%) FPD[4]	13 (45%) II[5]	15 (39%) (14- FPD; 1- II)	2 (17%) FPD
Siemens	–	3 (4%) II	10 (34%) (5- FPD; 5- II)	9 (24%) FPD	3 (25%) FPD
GE	3 (25%) II	33 (87%) II	5 (18%) II	4 (11%) FPD	--
Toshiba	–	–	1 (3%) II	10 (26%) FPD	7 (58%) FPD
Ziehm	–	1 (1%) II	–	–	–
Hologic	6 (50%) II	–	–	–	–
Orthoscan	3 (25%) II	–	–	–	–
[1]interventional radiology (IRR) [2]interventional cardiology (IRC) [3] electrophysiology (EP) [4] flat panel detector (FPD) [5] image intensifier (II)					

2.1 Participating Sites and Equipment

Table 1 shows the distribution of equipment manufacturers surveyed across all sites. Of the 16 surveyed sites, 9 were dedicated, free-standing pediatric medical centers, 6 were either adult-oriented facilities with available pediatric services or primarily adult-oriented facilities in rural communities, and one site was at the manufacturer's headquarters. Fluoroscopes at adult-oriented facilities were used on both adult and pediatric patients. Seven fluoroscopic vendors were represented in this study (Table 1). Only one dedicated pediatric hospital indicated the use of fluoroscopic units specifically configured for pediatric patients. The manufacture date for most of the fluoroscopic equipment included in this report ranged from 2005 to 2017.

The general fluoroscopic (GF) units had under-table x-ray tubes with over-table image receptors. Remote units with an under-table image receptor and an over-table x-ray tube were excluded, as were mobile O-arm units.

2.2 Measurement Protocol

Measurements were made with readily available, inexpensive materials to facilitate incorporation into a quality control program. Table 2 summarizes the protocols for each type of fluoroscope. For units with an image intensifier (II) input mode, measurements were made with the field of view (FOV) that was nearest to 23 cm (9 in). Measurements on flat-panel detectors (FPD) were made with the FOV closest to 20×20 cm. The available FOV varied by unit for mini C-arms, but either a 15-cm or a 10-cm FOV was evaluated.

AKR measurements were made at the entrance of seven different PMMA thicknesses, ranging from 1.25 to 25 cm. As shown in Table 3, the pediatric extremity AKR measurements were made using 1.25, 2.5, and 5 cm of PMMA, which correspond to the average sizes of the radius/ulna in a 1- to 2-year-old, 7- to 8-year-old, and 16- to 17-year-old pediatric patient, respectively. The 5-cm slab also represents the average adult hand thickness. The phantom thicknesses of 10, 15, 20, and 25 cm represent, respectively, an average newborn's trunk, an 8-year-old's trunk, a 17-year-old's trunk, and an adult trunk, as shown in Table 3. All PMMA slabs had 25×25 cm cross-sections.

Both solid-state and ionization chamber dosimeters were used. All dosimeters were calibrated via a NIST-traceable laboratory. Since ionization chamber dosimeters record backscatter from the PMMA, a backscatter factor of 1.35 (Wagner et al. 2000, Wunderle et al. 2017) was applied to solid-

Table 2: Mode of Operation for Each Type of Fluoroscope
(Both fluoroscopic and fluorographic operating modes were evaluated
using automatic dose rate control, ADRC.)

Parameter	Mini C-arm	Mobile C-arm	Gen Fluoro[9] (GF)	IRR[6]	IRC[7]	EP[8]
Exam	Extremity	Abdomen	GI	Abdomen	Thorax	Thorax
PMMA Thickness (cm)	1.25, 2.5, 5	5, 10, 15, 20, 25	5, 10, 15, 20, 25	5, 10, 15, 20, 25	5, 10, 15, 20, 25	5, 10, 15, 20, 25
Con vs Pulse	Con	Con & Pulsed	Pulsed	Pulsed	Pulsed	Pulsed
Dose Level	Normal[1]	Normal[1]	Normal[1]	Normal[1]	Normal[1]	Normal[1]
Added Filter	Std[9]	Std[9]	Var	Var	Var	Var
FOV (cm)	15 or 10	23[3]	23[3]	23[3]	23[3]	23[3]
Source to Chamber Distance (cm)	35	70	Var[2]	70	70	70
Source to Image Receptor Distance (cm)	44	100	~85[4]	100	100	100
Phantom entrance (cm)	SCD + 2	SCD + 4	SCD + 4	SCD + 4	SCD + 4	SCD + 4
Pulse Rate (P/s) Fluoroscopy	Con	Con & 7.5	7.5	15	15 & 30	7.5
Pulse Rate (P/s) Fluorographic	Single	Single	2	3	15 & 30	7.5
Presentation Fluorographic	DA	DA	DA	DSA	DA	DA
Grid	No	Yes	No 5 & 10 Yes 15, 20, 25	No 5 & 10 Yes 15, 20, 25	No 5 & 10 Yes 15, 20, 25	No 5 & 10 Yes 15, 20, 25

[1]Routine image receptor dose level used for nominal aged child imaged. See Table 4.
[2]Variable among GF units, ranges from ~50 to 65 cm.
[3]Area of image intensifier ~410 cm^2; FOV of flat panel closest to 410 cm^2; approximately 20 cm dimension
[4]Image receptor cover to be positioned 30 cm above the table top.
[5]SCD – source-to-chamber-surface distance
[6]IRR – interventional radiology unit
[7]IRC – interventional cardiology unit
[8]EP – electrophysiology unit
[9]2.5 to 3 mm Al total equivalent filtration; ~3 mm Al measured half value layer at 80 kVp
Con – continuous
Std – standard
Var – variable; 1 mm Al plus 0.1–0.9 Cu added; 3–8 mm Al measured half value layer
Gen Fluoro – general fluoroscopy

Table 3: Modeled Patient Thickness
(Kleinman 2010)

Patient Category	Nominal PMMA Thickness (inches)	(cm)
Ave newborn extremity	0.5	1.25
Ave 8-yr-old extremity	1	2.5
Ave 17-yr-old extremity	2	5
Ave newborn trunk	4	10
Ave 8-year-old trunk	6	15
Ave 17-year-old trunk	8	20
Ave adult trunk	10	25

Figure 1. Measurement geometry and general equipment setup for (a) mini C-arms, (b) mobile C-arms (slabs of PMMA placed directly on the input II or FPD), (c) general fluoroscopes (GF), (d) interventional angiographic radiology (IRR), interventional cardiac (IRC), and electrophysiology (EP) equipment.

state meter measurements to compare measurements made with both types of meters. All-solid-state dosimeters were placed toward the outer edge of the FOV to minimize the extent to which a lead-backed dosimeter could cause the AKR to increase. Consistent with Image Gently guidelines (IGA 2014c) and to further standardize the data collection protocol, the anti-scatter grid was removed for PMMA thicknesses of 10 cm or less (Table 2).

Whenever possible, a source-to-image-receptor distance (SID) of 100 cm was used. For GF units with a fixed source-to-skin distance (SSD), the image receptor was placed 30 cm above the tabletop. The measured AKR was reported in AK/time (mGy/min) for the fluoroscopic mode and AK/pulse (mGy/p) for the fluorographic modes. In Table 2, the pulse rate in the fluorographic mode ranged from single image to 30 P/s, depending on the type of fluoroscope. The presentation of the fluorographic images, i.e., digital subtraction angiography (DSA) versus digital angiography (DA), which is a non-subtracted presentation, is also dependent on the type of fluoroscope evaluated. The maximum output of each fluoroscopic unit was also measured to ensure that each unit complied with regulatory maximum output standards.

The measurement geometry adopted by the TG for each fluoroscope is illustrated in Figure 1. All possible variables in the measurement protocol could not be anticipated for every unit in the installed base. In these situations, the QMPs were asked to adopt the settings that most closely resembled the clinical situation for an average-aged child, as shown in Table 2.

2.3 Statistical Analysis

All plots and analyses were generated with RStudio (RStudio, Inc., Boston, MA, version 1.1.423). Box plots used in this report compare the distribution of measured or documented parameters. Each box's upper and lower boundaries represent the third and first quartile; the centerline is the median value. The whiskers represent 1.5 times the standard deviation of the data.

Violin plots were used to outline the kernel probability density. The width of the shaded area in each plot illustrates the proportion of AKR values located at that level for each phantom thickness. The violin plots also contain box plots. The non-parametric Mann-Whitney U test was used to test the null hypothesis that the mean rank of the AKR measurements across all phantom thicknesses between pediatric and adult IRC facilities is not equal. The "N-1" Chi-squared test was used to compare differ-

ences in percentages, where the null hypothesis indicates no difference. Both tests used a significance level of $\alpha = 0.05$, with a P-value greater than 0.05, suggesting rejection of the null hypothesis.

3. Results

3.1 Equipment Surveyed

A total of 131 fluoroscopic systems were evaluated. Table 4 summarizes the number and types of fluoroscopic equipment surveyed by hospital type: adult hospital or pediatric hospital. Evaluations performed at a manufacturers' headquarters are included in the adult facility category.

3.2 Incident Air Kerma Rate (AKR)

Interventional fluoroscopic units accounted for 38 of the 131 units surveyed; 18 (13.7%) and 20 (15.2%) of these 131 units were used for IRR and IRC applications. The AKRs collected for the IRC and IRR fluoroscopic modes are compared in Figure 2. The data in this figure illustrate that the fluoroscopic AKRs may differ for similar interventional fluoroscopic units depending on the clinical application. The IRC fluoroscopes had a lower median AKR than the IRR fluoroscopes at all phantom thicknesses for a number of reasons. First, the IRC fluoroscopes were evaluated using a thorax exam configuration designed for cardiac studies, while IRR fluoroscopes were evaluated using an abdominal or neuro exam configuration. Variation in the unique nominal focal spot size, selected voltages, available tube current, pulse rate, pulse width, and thickness of filtration added in the x-ray beam are just some of the configurable parameters that affect the AKR. Third, less radiation is required to penetrate the thorax than the abdomen or head (soft tissue and air-filled lungs vs soft tissue or solid soft tissue and bone). Finally, the configured AKR at the entrance plain of the image receptor may be different for the two different clinical applications. Six of the IRC units with novel image processing (30% of the submissions in this study) were configured with substantially reduced AKR values at the image receptor, which reduced the study's AKR for IRC units. This reduced AKR at the image receptor, set up by the QMP with cooperation of the equipment vendor, was possible due to the unit's advanced image processing and the cardiologists' tolerance for increased quantum mottle levels in the image.

Table 4: The Number of Fluoroscopic Units Evaluated by Clinical Setting and Type

Clinical Setting	Number of Units Evaluated						
	Mini C-arm	Mobile C-arm	General Fluoro	IRR[1]	IRC[2]	EP[3]	Total
Adult hospital	1	20	9	5	10	7	52
Pediatric hospital	11	20	20	13	10	5	79

[1] IRR – interventional angiographic radiology unit
[2] IRC – interventional cardiology unit
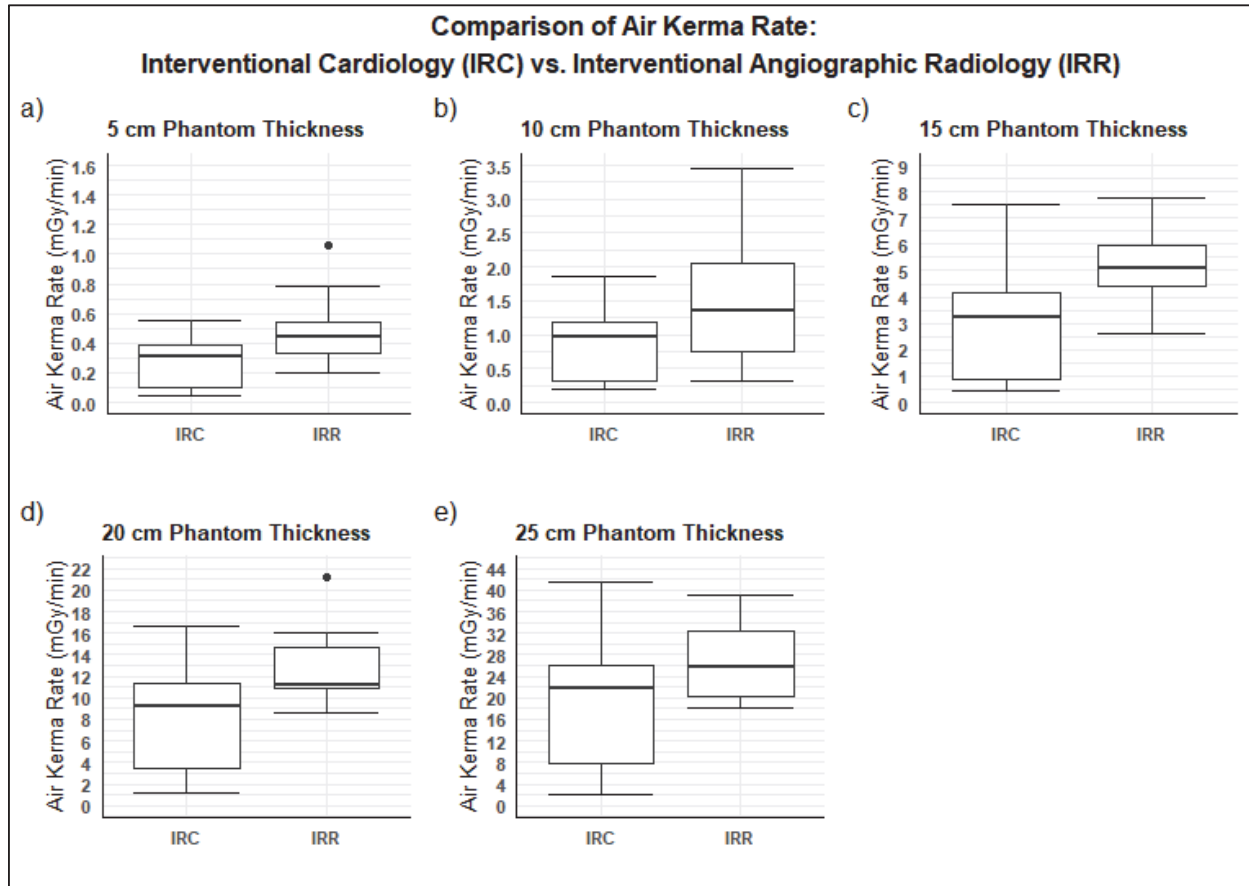[3] EP – electrophysiology unit

Figure 2. Distribution of incident air kerma rates (AKRs) as a function of phantom thicknesses for interventional cardiology (IRC) (N = 20) and interventional radiology (IRR) (N = 18) fluoroscopes. Data collected for IRC units were obtained with a thorax exam protocol with 15 p/s. The IRR units were measured using an abdominal exam protocol with 15 p/s. **Please note that the scale of the ordinate for each pair of box plots is unique**.
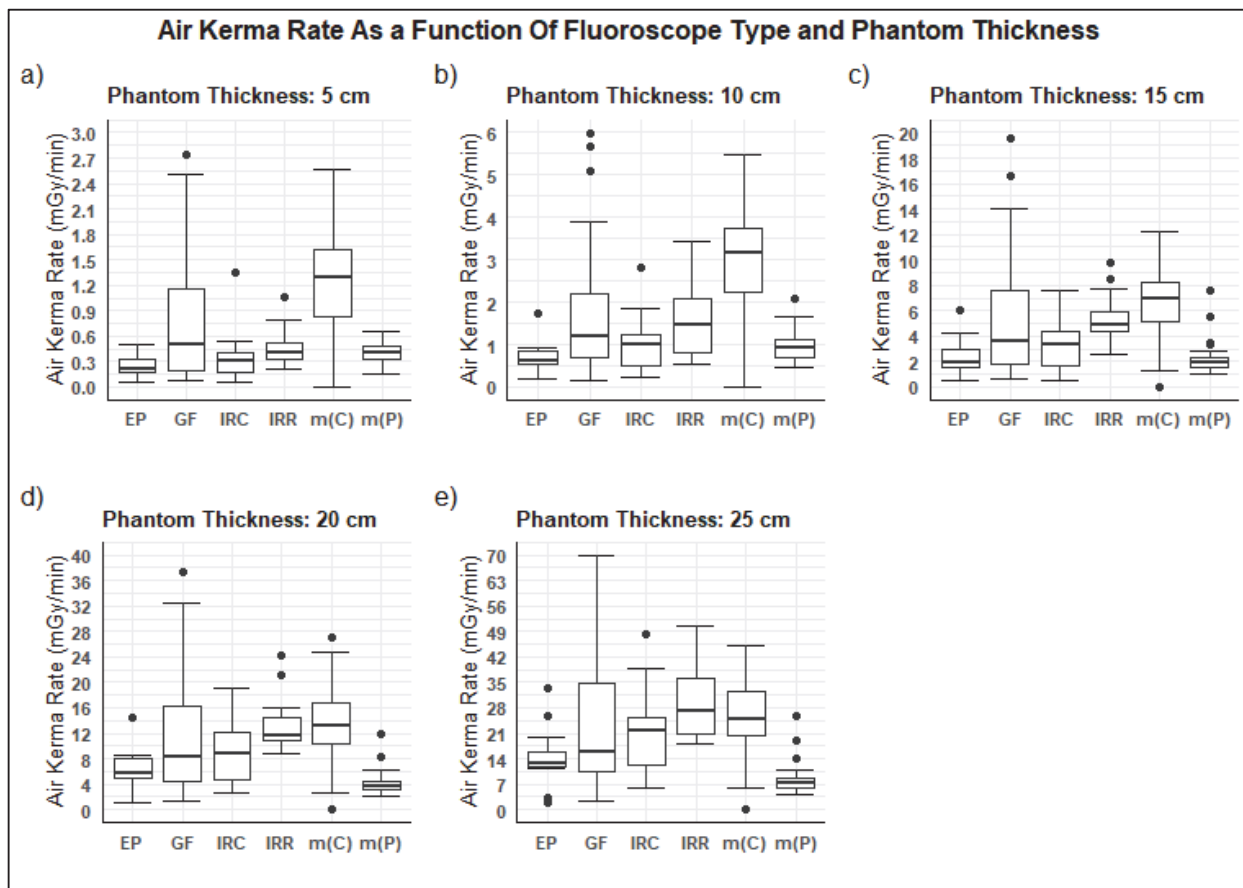
Figure 3. Distribution of incident air kerma rates (AKRs) for each fluoroscope, evaluated as a function of phantom thickness. EP = cardiac electrophysiology labs, GF = general fluoroscopes, IRC = cardiac IR, IRR = interventional angiographic radiology, M(C) = continuous mode of mobile fluoroscope, M(P) = pulsed mode of the mobile fluoroscope. The frame rates for each type of unit are as specified in Table 2. **Please note that the scale of the ordinate for each set of box plots is unique.**

Figure 3 shows the distribution of AKR with increasing phantom thickness for each type of fluoroscope evaluated across adult and pediatric sites, except for mini C-arms. While some variation in the median AKR is illustrated within each individual phantom thickness for the EP, GF, IRC, and IRR units, the differences are not large. For the phantom thicknesses greater than 15 cm, the AKR of the mobile fluoroscopes in the pulsed mode are approximately half of the values of GF units. However, in the continuous mode of the mobile fluoroscopes, the AKR is more than 3 times greater than the AKR in the pulsed mode (8 p/sec).
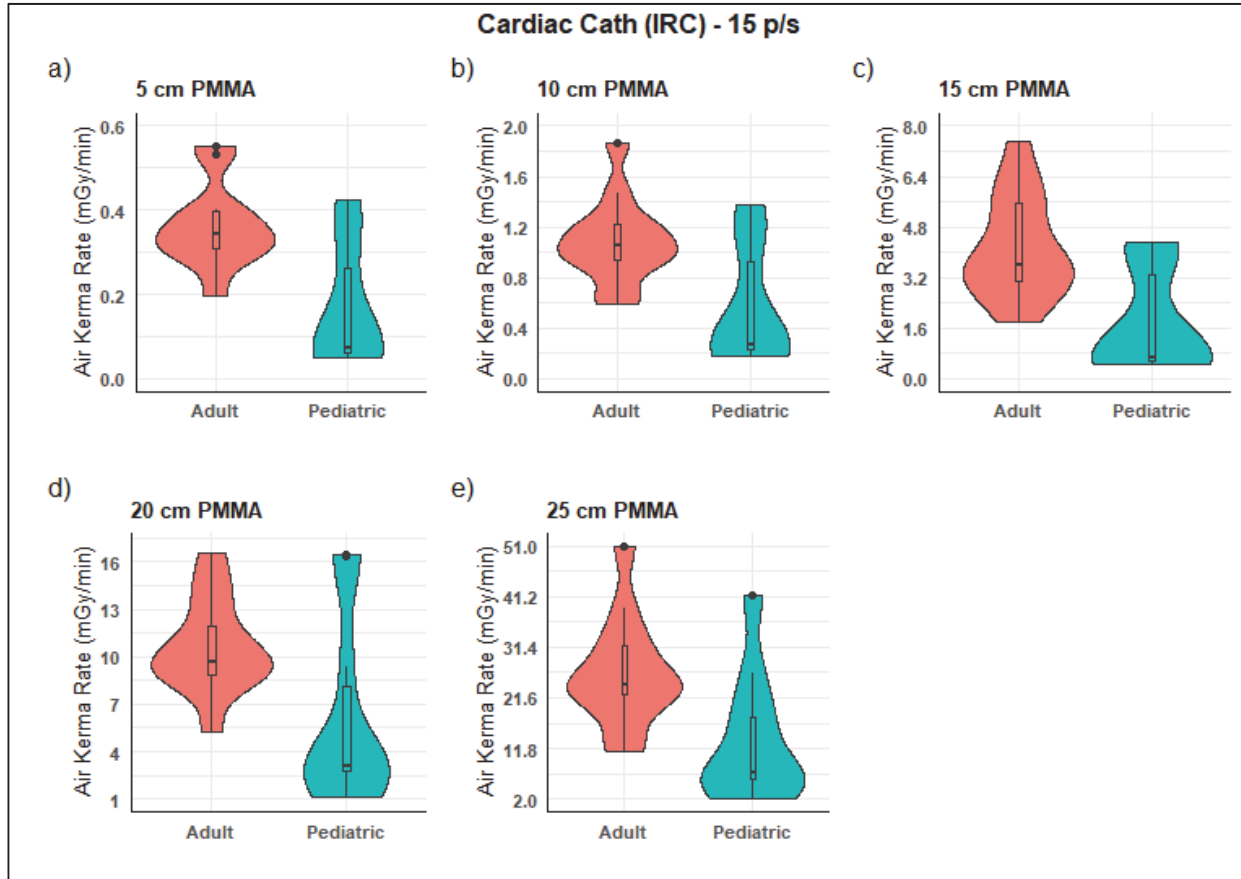
Figure 4-I. Measured incident air kerma rates (AKR) from adult and pediatric cardiac cath labs (IRC) (N = 10 for both). **Please note that the scale of the ordinate for each pair of violin plots is unique.**

Figures 4-1 to 4-6 display violin plots that compare AKR between adult and pediatric medical centers. For GF, EP, and mobile C-arms both pulsed and continuous, fluoroscopes at dedicated pediatric medical centers had median AKR values lower than fluoroscopes at adult medical centers. This trend was more pronounced for IRC units.

Figure 4-2. Distribution of measured incident air kerma rates (AKR) from adult and pediatric interventional radiology (IRR) fluoroscopes (N = 5 and 13, respectively). **Please note that the scale of the ordinate for each pair of violin plots is unique.**
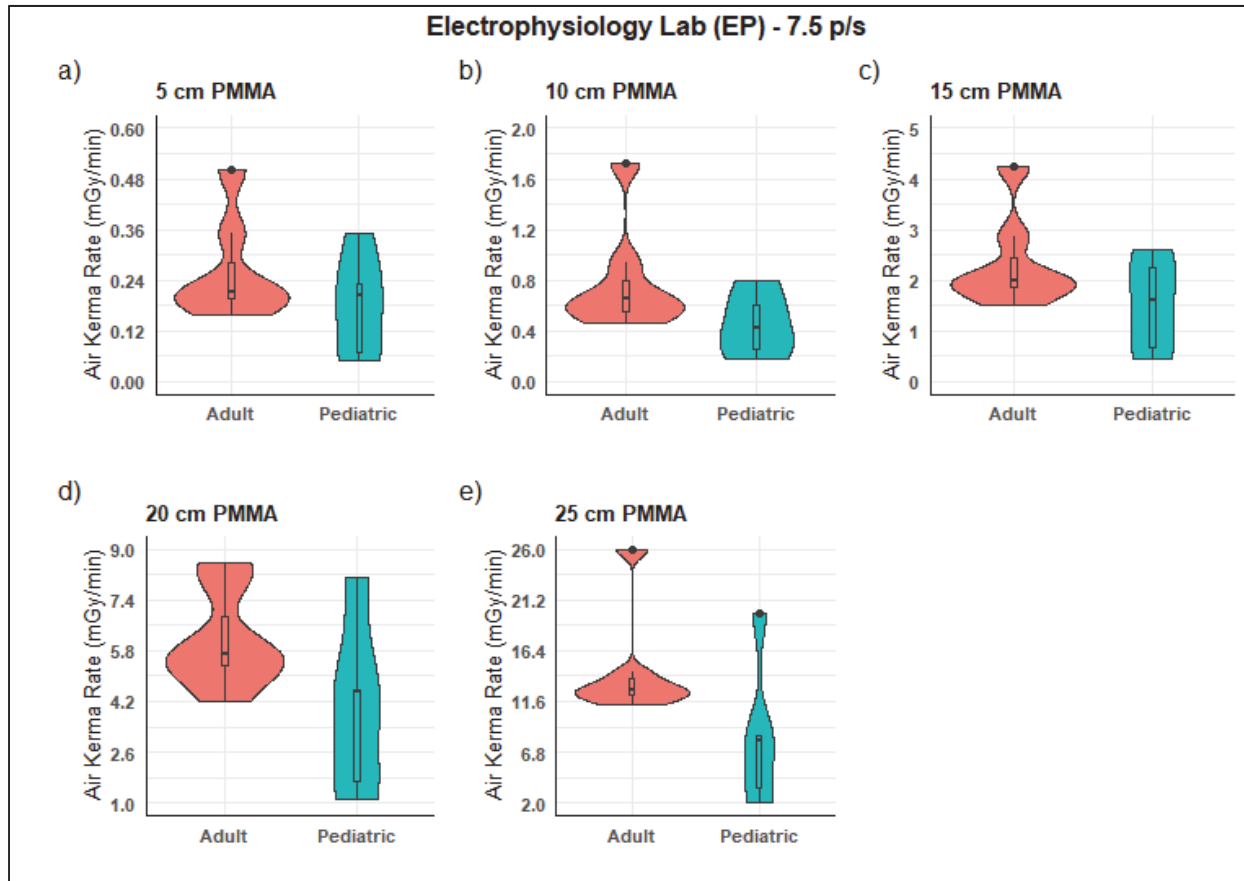
Figure 4-3. Distribution of measured incident air kerma rates (AKR) from adult and pediatric electrophysiology (EP) labs (N = 7 and 5, respectively). **Please note that the scale of the ordinate for each pair of violin plots is unique**.
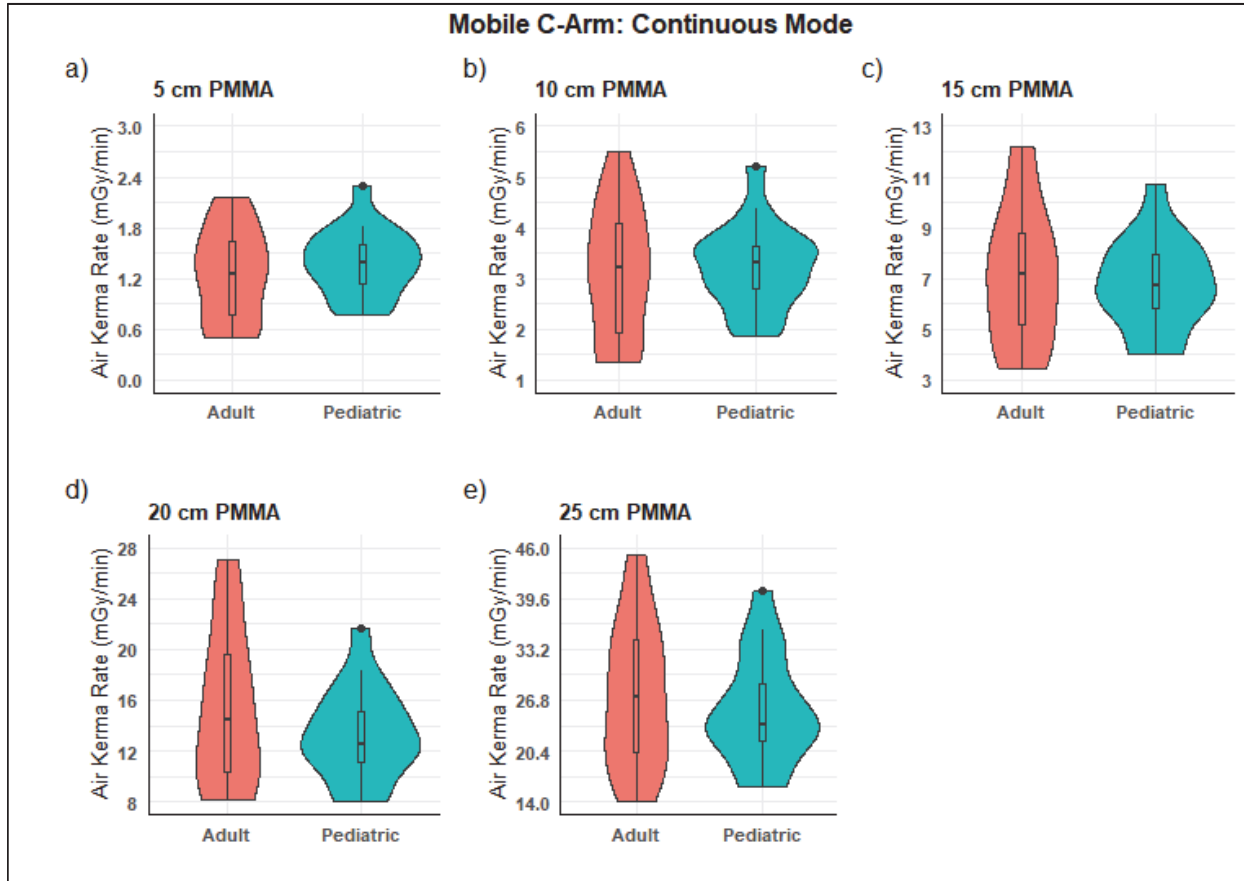
Figure 4-4. Distribution of measured incident air kerma rates (AKR) from adult and pediatric mobile C-arms operated in the continuous mode (N = 20 for both). **Please note that the scale of the ordinate for each pair of violin plots is unique**.

Figure 4-5. Distribution of measured incident air kerma rates (AKR) from adult and pediatric mobile C-arms (N = 16 and 20, respectively). **Please note that the scale of the ordinate for each pair of violin plots is unique.**
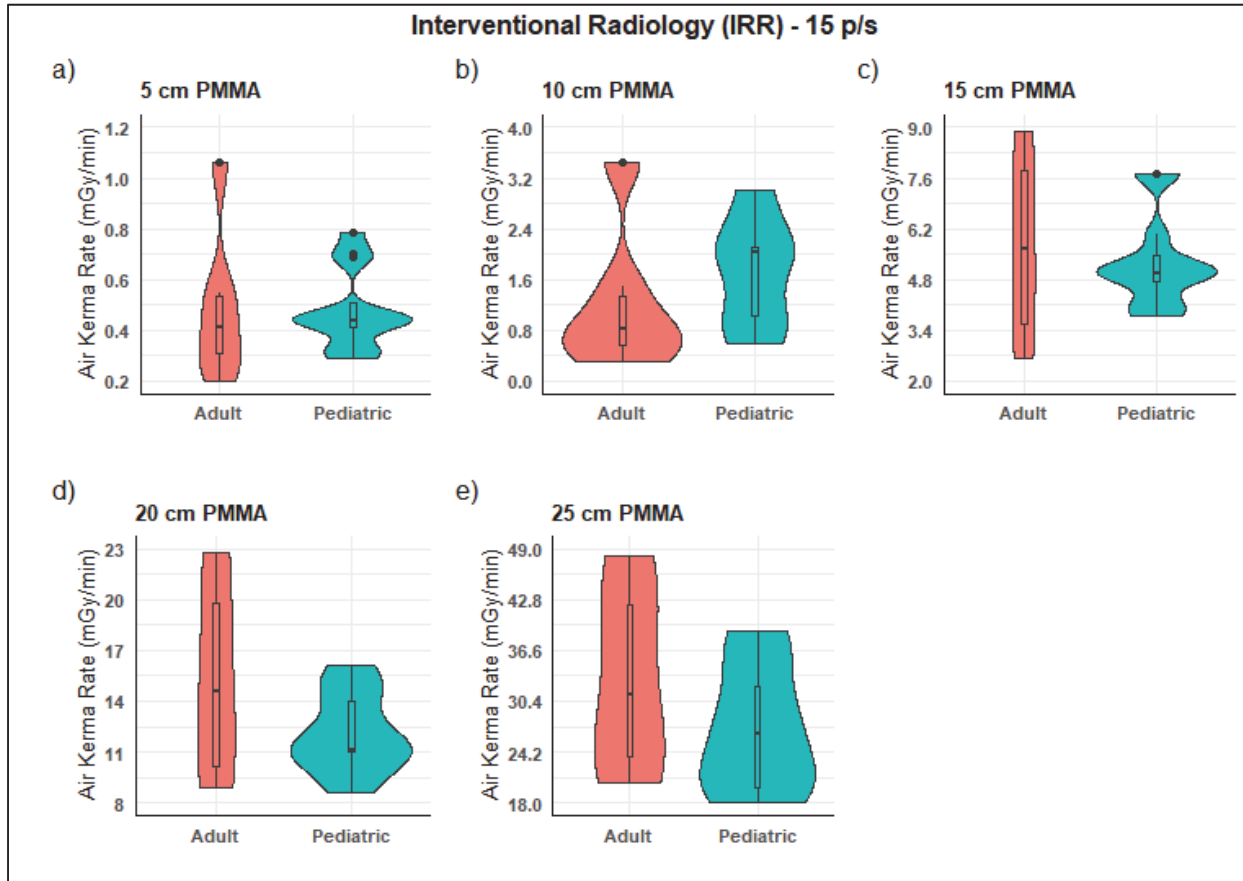
Figure 4-6. Distribution of measured incident air kerma rates (AKR) from adult and pediatric general fluoroscopes (GF) (N = 9 and 20, respectively). **Please note that the scale of the ordinate for each pair of violin plots is unique**.

Table 5: Fluoroscopic Mode
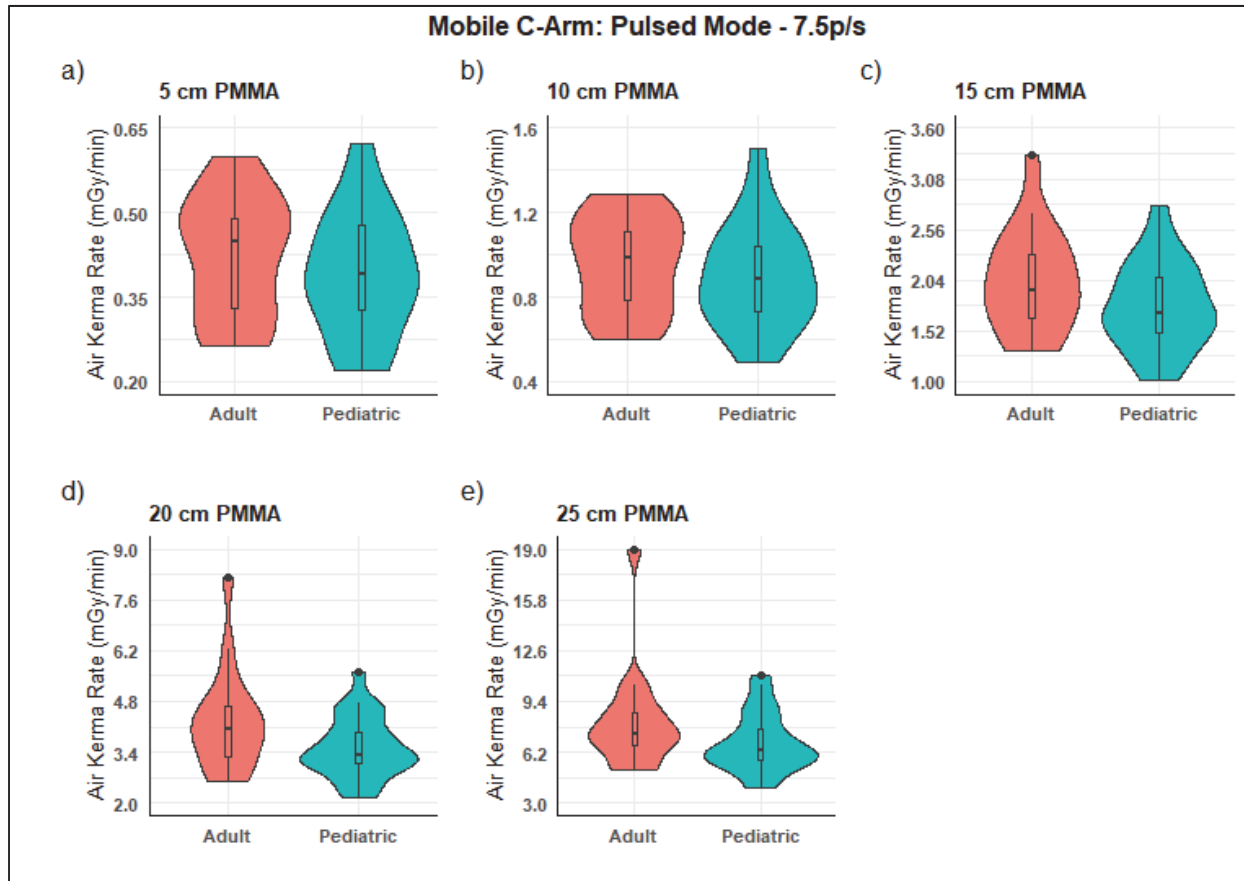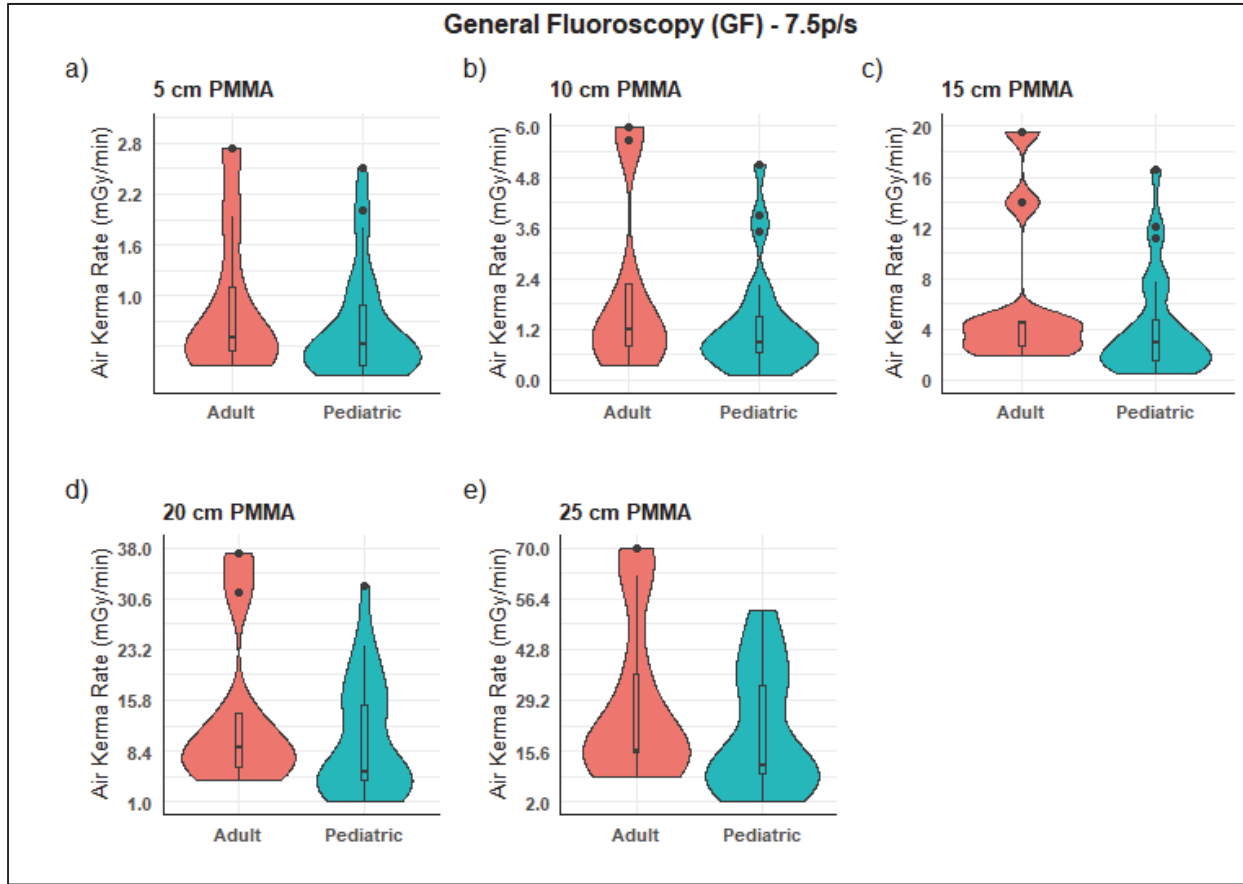Median, 25th, and 75th percentile values for the fluoroscopic incident air kerma rate (AKR) measured with each phantom thickness. All AKR values are specified in mGy/min at the source-to-chamber distance (SCD) of 50–65 cm for GF units and 70 cm for all other types of units. The frame rates for each type of unit in the first three rows are mixed, as specified in Table 2.

System Type	Thickness (cm)				
	5	10	15	20	25
Across all fluoroscopic systems	0.435 (0.285, 0.776)	1.11 (0.716, 2.08)	3.58 (1.88, 5.92)	8.67 (4.19, 14.4)	19.9 (8.53, 29.4)
Across systems located at adult facilities	0.484 (0.315, 0.593)	1.20 (0.844, 1.74)	3.78 (2.39, 5.85)	8.88 (5.68, 14.83)	22.4 (12.5, 31.5)
Across systems located at dedicated pediatric facilities	0.443 (0.228, 0.832)	1.05 (0.663, 2.15)	2.98 (1.58, 5.93)	7.02 (3.24, 14.2)	15.9 (6.53, 27.9)
General Fluoroscope (GF) 7.5 p/s	0.432 (0.193, 0.945)	1.07 (0.682, 1.63)	3.09 (1.82, 4.73)	6.21 (4.23, 15.1)	14.1 (9.66, 34.2)
Mobile C-arms Continuous Mode	1.29 (0.834, 1.62)	3.15 (2.24, 3.75)	6.73 (5.14, 8.23)	12.52 (10.3, 16.8)	23.7 (20.2, 32.3)
Mobile C-arms Pulsed Mode 7.5 p/s	0.395 (0.331, 0.484)	0.911 (0.713, 1.10)	1.86 (1.60, 2.25)	3.70 (3.18, 4.50)	7.03 (5.80, 8.70)
Interventional Radiology (IRR) 15 p/s	0.443 (0.336, 0.543)	1.35 (0.751, 2.06)	5.08 (4.38, 5.95)	11.63 (10.9, 15.2)	27.0 (20.6, 36.1)
Interventional Cardiology (IRC) 15 p/s	0.309 (0.099, 0.387)	0.954 (0.312, 1.19)	3.25 (0.897, 4.15)	9.16 (3.39, 11.4)	22.04 (8.74, 26.3)
Interventional Cardiology (IRC) 30 p/s	0.442 (0.362, 0.575)	1.34 (0.876, 1.76)	4.60 (3.77, 7.95)	15.5 (12.1, 20.1)	29.9 (28.8, 40.4)
Electrophysiology (EP) 7.5 p/s	0.206 (0.163, 0.249)	0.582 (0.421, 0.694)	1.88 (1.58, 2.17)	5.35 (3.98, 6.28)	12.2 (7.46, 13.5)

Table 5 lists the median, 25th, and 75th percentile AKRs measured in the fluoroscopic mode (mGy/min) for all fluoroscopes as a function of phantom thickness. The fluoroscopic AKRs for units in pediatric facilities were less than in adult facilities at each measured phantom thickness. The measurement protocol detailed in Table 2 called for AKR measurements to be repeated for 30 p/s in addition to 15 p/s for the IRC units. During the period when the data of this study was collected, 15 p/s fluoroscopy for pediatric cardiac interventions in the United States began to be substituted for 30 p/s data as pediatric cardiologists accepted the reduced temporal resolution of 15 p/s fluoroscopy in an effort to reduce the total patient radiation dose during cardiac interventions. The fluoroscopic AKR (mGy/min) in Table 5 for 30 p/s is greater than 15 p/s data, which is greater than fluoroscopy in EP Labs, which is performed at 7.5 p/s.

Table 6: Fluorographic Mode
Median (25th and 75th percentile) and [N] values for fluorographic incident air kerma rate (AKR) value
measured with each phantom thickness and stratified by institution type, either adult or pediatric.
All AKR are specified in mGy/pulse at the source-to-chamber distance (SCD)
of 50–65 cm for GF units and 70 cm for all other types of units.

System Type	Institution Type [# of units]	Thickness (cm)				
		5	10	15	20	25
General Fluoroscope (GF) 2.0 p/s	Adult [5]	0.07 (0.034, 0.07)	0.099 (0.093, 0.17)	0.372 (0.186, 1.04)	0.944 (0.481, 3.06)	2.33 (0.918, 7.71)
	Ped [20]	0.014 (0.003, 0.03)	0.051 (0.003, 0.06)	0.944 (0.481, 3.06)	0.3 (0.043, 0.403)	0.652 (0.059, 0.91)
Mobile C-arms Single shot	Adult [6]	0.03 (0.023, 0.331)	0.102 (0.085, 0.343)	2.33 (0.918, 7.71)	0.48 (0.465, 0.533)	1.101 (0.673, 1.468)
	Ped [3]	0.025 (0.023, 0.054)	0.147 (0.106, 0.189)	0.014 (0.003, 0.03)	0.305 (0.273, 0.441)	0.6 (0.52, 0.684)
Interventional Radiology (IRR) 3 p/s	Adult [2]	0.067 (0.039, 0.096)	0.166 (0.098, 0.233)	0.051 (0.003, 0.06)	1.37 (1.035, 1.705)	3.625 (2.713, 4.538)
	Ped [9]	0.028 (0.021, 0.039)	0.082 (0.068, 0.11)	0.13 (0.01, 0.218)	0.678 (0.528, 0.924)	1.74 (1.364, 3.01)
Interventional Cardiology (IRC) 15 p/s	Adult [20]	0.002 (0.002, 0.006)	0.006 (0.005, 0.015)	0.3 (0.043, 0.403)	0.08 (0.06, 0.125)	0.3 (0.258, 0.343)
	Ped [8]	0.001 (0.001, 0.002)	0.004 (0.003, 0.011)	0.652 (0.059, 0.91)	0.04 (0.035, 0.102)	0.126 (0.088, 0.233)
Electrophysiology (EP) 7.5 p/s	Adult [7]	0.003 (0.002, 0.012)	0.01 (0.008, 0.093)	0.03 (0.023, 0.331)	0.13 (0.07, 0.83)	0.33 (0.275, 1.235)
	Ped [4]	0.004 (0.002, 0.007)	0.004 (0.004, 0.007)	0.102 (0.085, 0.343)	0.038 (0.026, 0.063)	0.081 (0.06, 0.125)

The data in Table 6 for the fluorographic mode is presented in units of mGy/pulse at the frame rates listed in the first column. For each type of unit, the results for adult and pediatric facilities are listed in separate rows. The last integer in square brackets for each entry is the sample size. With the exception of mobile c-arms with the 10-cm phantom, the AKR in the fluorographic mode for all units in pediatric facilities was less than the AKR in adult facilities. Since the data in this table is presented as AK/pulse, the values in the table are independent of the pulse rate during the measurement, which allows the 15 and 30 p/s data for IRC to be mixed together. As expected, the measured values of the IRR units using DSA were 10–20 times greater than the measured values in the IRC using DA.

Table 7: Mini C-arm
Median and interquartile range values for fluoroscopy and fluorographic incident air kerma rate (AKR) measured with each phantom thickness. Fluoroscopic and fluorographic AKRs are expressed in units of mGy/min and mGy/pulse, respectively, at the source-to-chamber distance (SCD) of 35 cm. The frame rates are as specified in Table 2.

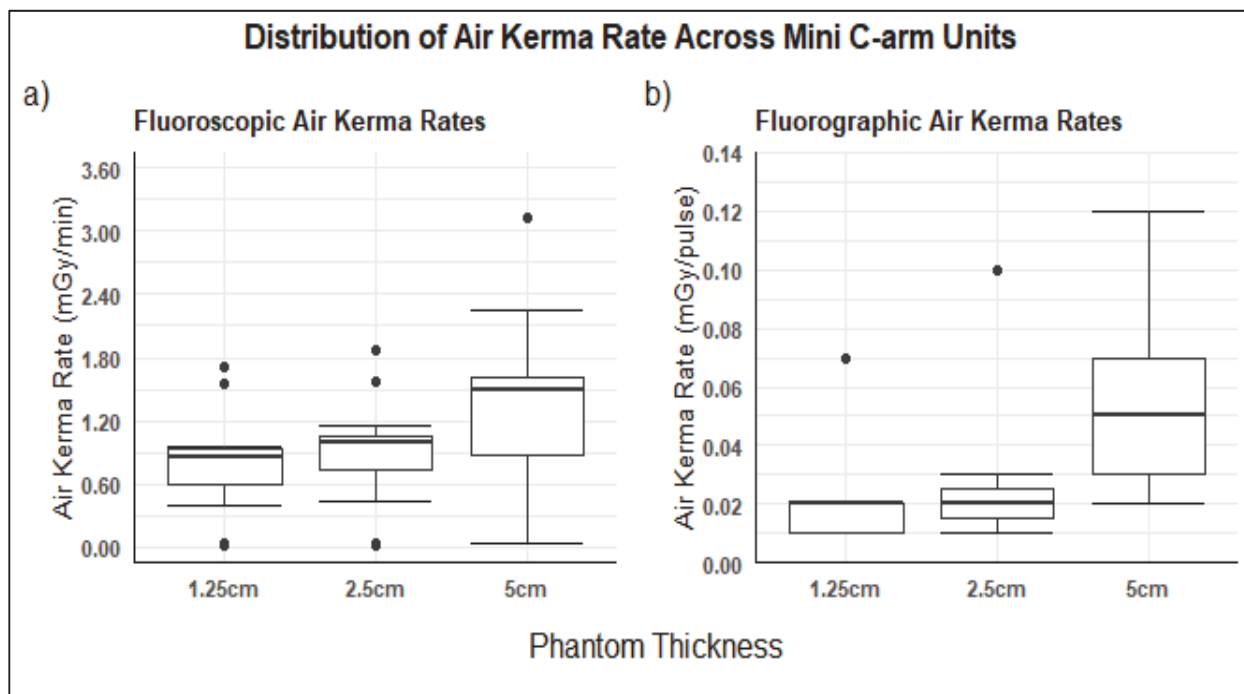| Thickness (cm)	Fluoroscopy (mGy/min)	Fluorographic (mGy/pulse)
1.25	0.855 (0.601, 0.944)	0.017 (0.011, 0.020)
2.5	0.993 (0.741, 1.051)	0.017 (0.015, 0.022)
5	1.500 (0.915, 1.639)	0.049 (0.029, 0.068)

Figure 5. (a) Box plots of fluoroscopic incident air kerma rate (AKR, mGy/min) for mini C-arm units operated in the continuous mode. (b) Box plots of fluorographic AKR (mGy/pulse). Note that the scale of the ordinate differs for (a) and (b).

Table 7 and Figure 5 show the distribution of AKR values collected for mini C-arms.

While the half-value layer (HVL) at 70 kV for an x-ray beam with standard (equivalent 2.5 mm Al) filtration with a measured HVL = 2.4 mm Al (at 70 kV) is approximately 3 cm of the patient thickness (Strauss, K. J. 2006a), the mean AKR doubled with each 4-cm increment of phantom thickness, regardless of the type of fluoroscope. This occurred for increased increments of phantom thickness that resulted in kV values greater than or equal to 80 kV.

Mini C-arms have been marketed for years as simpler units that deliver less radiation dose to the patient than standard fluoroscopes. Mini C-arms are simpler to operate because of the reduced number

Table 8: Reduction in incident air kerma rate (AKR) relative to the largest
phantom size of 25 cm when operated in the fluoroscopic mode

Phantom Thickness (cm)	IRC 15 p/s	EP 7.5 p/s	IRR 15 p/s	GF 7.5 p/s	m(C)	m(P) 7.5 p/s	Total Average % Across Rows
25	–	–	–	–	–	–	–
20	58.5%	56.4%	54.7%	51.0%	45.8%	48.1%	52.4%
15	85.1%	83.5%	81.2%	78.9%	73.7%	74.6%	79.5%
10	95.9%	94.6%	94.6%	93.3%	87.9%	87.7%	92.3%
5	98.7%	98.1%	98.3%	97.0%	94.9%	94.7%	97.0%

IRC – interventional cardiology unit
EP – electrophysiology
IRR – interventional angiographic radiology unit
GF – general fluoroscope
m(C) – continuous mode mobile C-arm
m(P) – pulsed mode mobile C-arm

output for mobile C-arms and mini C-arms (Table 7), using a 5-cm-thick PMMA phantom, indicate that the mini C-arms deliver higher mean AKRs. Mini C-arm fluoroscopy rates are 1.2 and 3.8 times greater than those for mobile C-arms operating in a continuous and pulsed mode, respectively. The single-shot AK of the mini C-arm is 1.6 times greater than that of the mobile C-arm. The increased AKR is partly due to the shorter SSD of the mini C-arm.

Table 8 lists the percent reduction of the measured AKR with reduced phantom thicknesses relative to the average-sized adult (25 cm phantom thickness) for each type of fluoroscope surveyed, excluding the mini C-arms. While some variation exists between the six types of fluoroscopes for a given phantom thickness, the reductions are similar. The last column of Table 8 lists the average reduction for each phantom thickness. This data, expressed as the median AKR represented by the solid black line of the whisker plots for each thickness phantom, is illustrated in Figure 6. As a first approximation, the median AKR approximately triples for small phantom thicknesses and doubles for larger phantom thicknesses each time the phantom thickness increases by 5 cm. Based on data in Figure 6, first order target values for the fluoroscopic median AKR of a fluoroscope are 0.5, 1.5, 4, 9, and 20 and 45 mGy/min for phantoms of thickness of 5, 10, 15, 20, 25 cm, and maximum output, respectively.
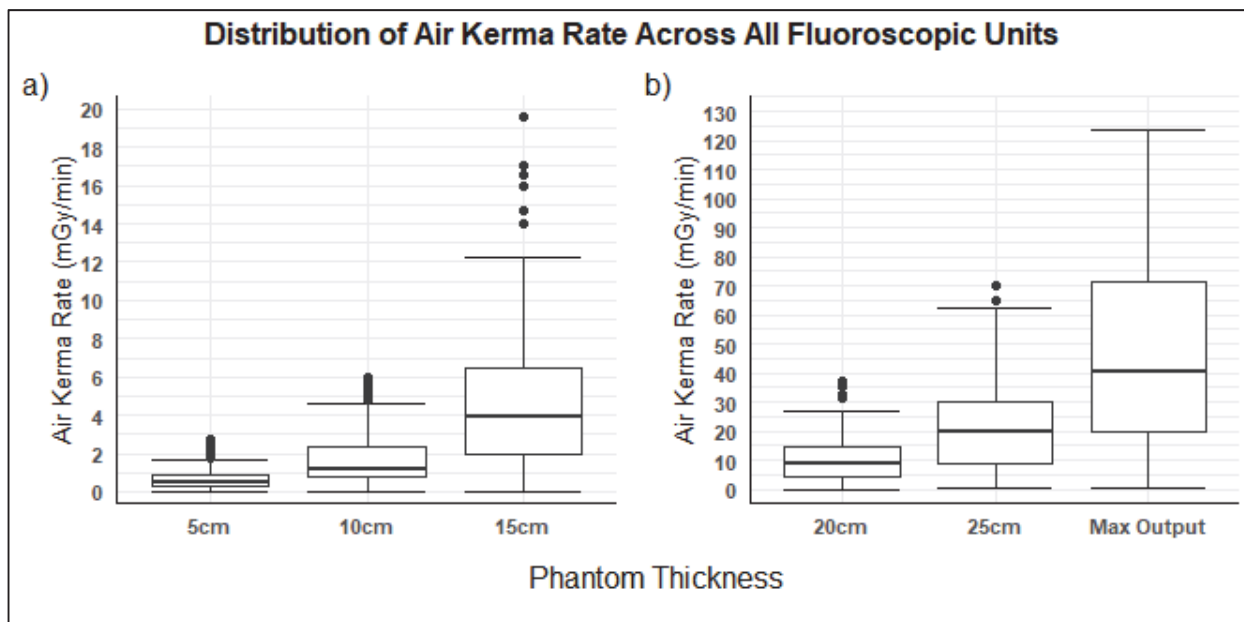
Figure 6. The incident air kerma rate (AKR) as a function of PMMA thickness is displayed for all 131 fluoroscopic units. (a) phantom thicknesses ranging from 5 to 15 cm and b) phantom thickness ranging from 20 cm to the max output. The upper and lower boundaries of each box represent the 3rd and 1st quartile, while the solid black line is the median. The whiskers represent 1.5 times the standard deviation of the data. Please note that the scale of the ordinate is different in (a) and (b). The frame rates for each type of are mixed, as specified in Table 2.

3.3 Tube Voltage and Pulse Width

The tube voltage and pulse width data displayed by the fluoroscopic systems were recorded and are displayed in Figures 7 and 8. The ways tube voltage and pulse width change as a function of phantom thickness illustrate some aspects of the control logic of a fluoroscope. For example, as phantom thickness increased from 5 to 25 cm, tube voltage increased moderately for the EP and IRC units from a median of 66 to 72 kV. However, for IRR units, mobile C-arms, and GF units, tube voltage increased from 56 to 98 kV for the same range of phantom thicknesses. The pre-programmed protocols for some EP and IRC units evaluated within this report were designed to maintain approximately 70 kV over a wide range of patient thicknesses to improve image contrast for the iodinated contrast agent. The maintenance of a similar kV over a moderate range of patient thicknesses differs by vendor and software versions. Physicists working with their vendors to optimize pediatric exam protocols of larger pediatric patients that utilize iodinated contrast should seek configurations designed to increase pulse width or the tube current with increasing patient thickness before increasing tube voltage. Likewise, pulse widths and tube current should be decreased for the smallest pediatric patients to maintain kV greater than 65 kV. Lower kV values for these small patients increase patient AKR values with little to no improvement in image quality (Strauss, K. J. 2000a).

Within tube power constraints, pulse widths used for pediatric fluoroscopy procedures should minimize motion blur. To maintain image sharpness and adequately visualize fast-moving organs such as the heart, maximum pulse widths of 5 and 10 msec are recommended for pediatric and adult patients, respectively (Strauss, K. J. 2006a; MITA 2015). For non-cardiac studies of large adults, maximum pulse widths of 15 msec may be necessary to penetrate the abdominal/pelvic region adequately. Figure 8 shows the distribution of pulse widths used by fluoroscopy systems included in this study
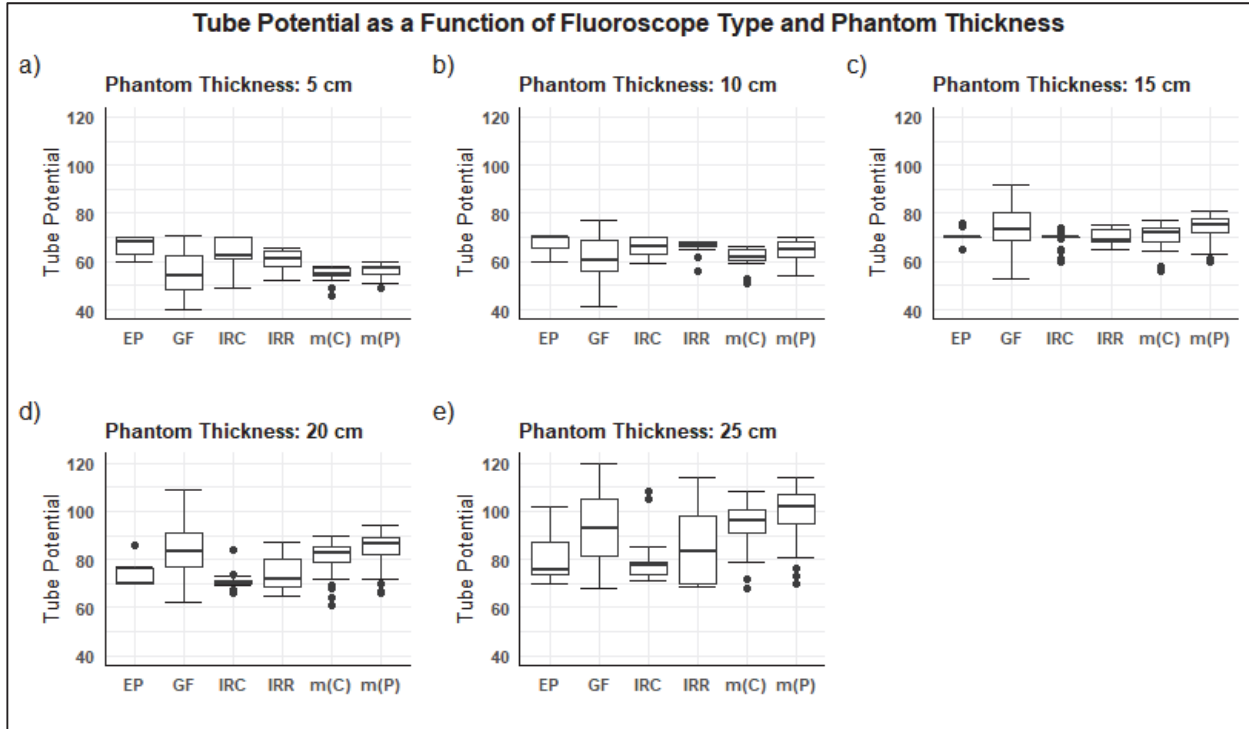
Figure 7. The distribution of kV as a function of PMMA thickness. EP = cardiac electrophysiology labs, GF = general fluoroscopes, IRC = cardiac IR, IRR = interventional radiology, M(C) = continuous mode of mobile fluoroscope, M(P) = pulsed mode of the mobile fluoroscope. The fluoroscopy mode frame rates are specified in Table 2.

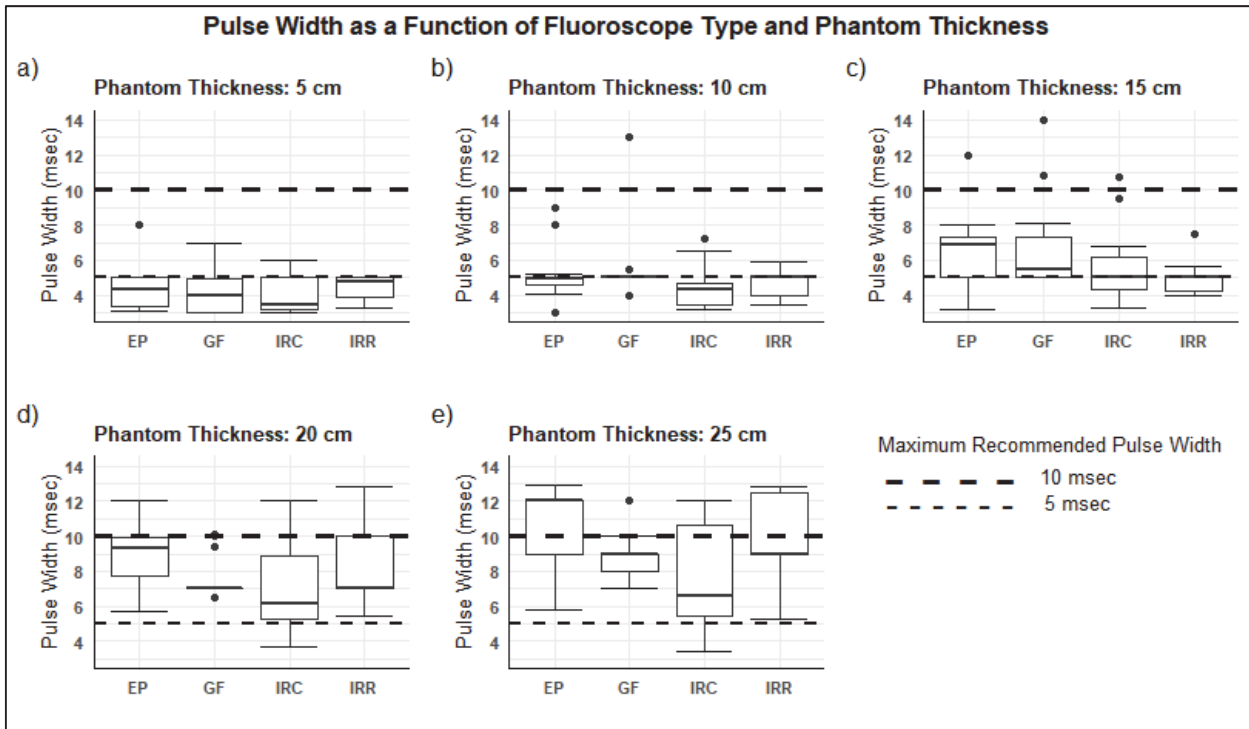

Figure 8. Pulse width, as displayed by the fluoroscopic systems. EP = cardiac electrophysiology labs, GF = general fluoroscopes, IRC = interventional cardiac IR, IRR = interventional radiology. The fluoroscopy mode frame rates are specified in Table 2. The dashed lines indicate the recommended maximum pulse widths for pediatric (5 msec) and adult (10 msec) patients (Strauss, K. J. 2006a).
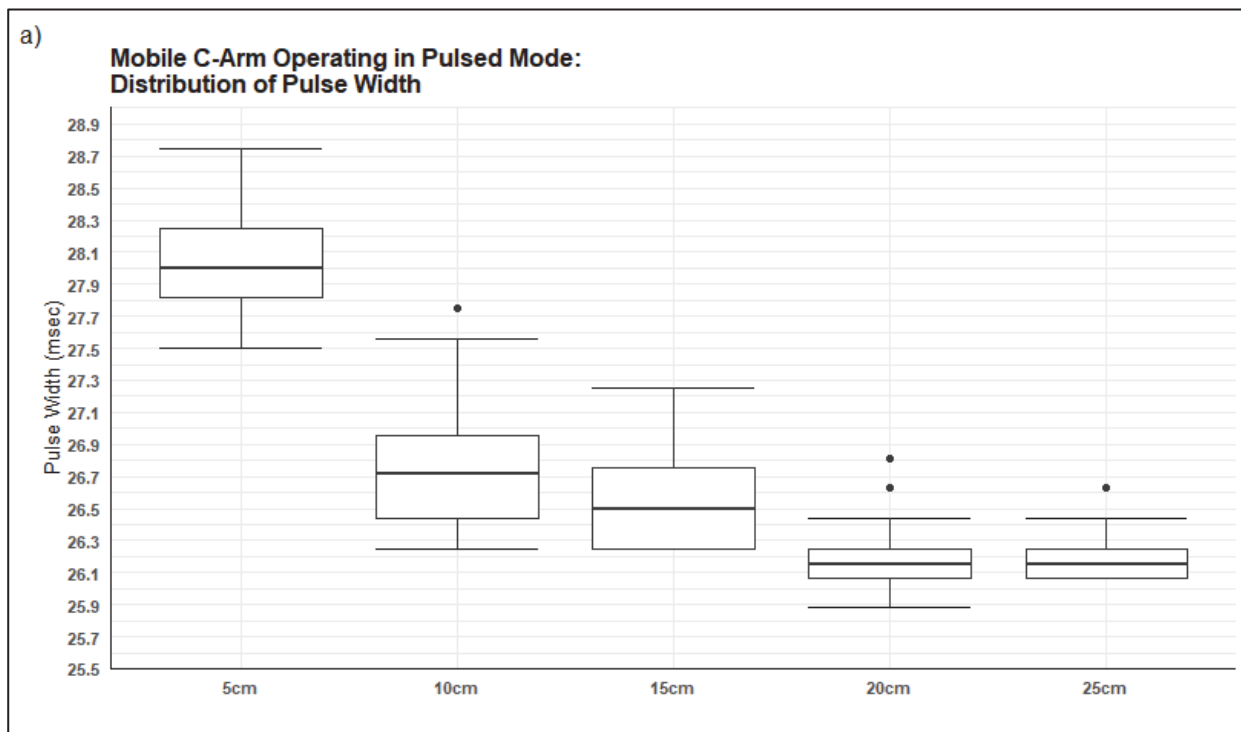
Figure 9. Pulse width distribution of a single manufacturer's mobile C-arms. The pulse width was calculated using solid-state waveform outputs.

sorted by equipment type and phantom thickness. For the 5 and 10 cm phantom thicknesses and for the 20 and 25 cm phantom thicknesses, ideally all units should have been configured to use pulse widths <5 msec and <10 msec, respectively. However, the data in Figure 8 illustrate that a number of units exceeded these recommended pulse widths.

The mobile C-arms evaluated in this survey did not display the pulse width. For the three major manufactures' units in this study—GE, Siemens, and Philips—the AKR waveform was collected with a solid-state dosimeter. The pulse width for each phantom thickness was estimated from the measured full-width-at-half-maximum of each waveform. Figure 9 illustrates the measured pulse widths from 26 to 29 msec. All of these mobile C-arm units use pulse widths that substantially exceeded the recommended maximum pulse widths of 5 and 10 msec for pediatric and adult patients, respectively (MITA 2015).

4. Discussion

The AAPM charged TG-251 with collecting and evaluating fluoroscopic and fluorographic AKRs as a function of simulated patient thicknesses to determine information about the state of the practice. The charge did not include an assessment of image quality. However, considering changes to image quality in conjunction with changes to air kerma is essential to clinical practice, particularly when evaluating or establishing air kerma reference ranges for quality control or clinical purposes. In any attempt to manage air kerma, image quality must also be appropriately assessed. This report outlines methods to manage fluoroscopy protocols for pediatrics, but does not diminish or should not be misconstrued to diminish the importance of evaluating and understanding image quality.

4.1 General Survey Outcomes

We developed a standard method to measure the AKR across phantom thicknesses that simulate patient sizes from an infant to adult (Kleinman 2010). If the fluoroscopic or fluorographic AKR for a given system exceeds the 75th percentile listed in Table 5 or 6, it is prudent to take further steps to examine the cause. Standardization of the measurement protocol enables QMPs to evaluate a fluoroscope's management of AKR as a function of patient size and to compare these measurements to other state-of-the-practice units. Considering the large number of variables in the conventional measurement of AKR, a standardized procedure facilitates meaningful comparisons.

The use of fluoroscopy on children requires additional considerations during the design and development of imaging protocols. The value of configuring fluoroscopic equipment protocols for pediatric-specific imaging tasks is noted in the statistically significant AKR reduction ($P < .001$) for IRC units operated at pediatric medical centers relative to adult medical centers, as seen in Figure 4-1. The lower AKR was due to the refinement of vendor-provided fluoroscopic protocols for the specific tasks and cardiologist preferences at a single pediatric institution included in this report. The process involved a close working relationship between the QMP and equipment vendor, careful evaluations of AKR across phantom sizes, advanced image processing applications, reduced pulse rates, and feedback from cardiologists about the adequacy of image quality with each reduction in AKR (Strauss K. J. 2019).

In contrast, the AKRs for fluoroscopes used for other clinical applications did not vary substantially between pediatric and adult centers. For example, Figure 4-6 for general fluoroscopes illustrated reductions of AKRs for units at pediatric sites, but the difference in the overall average AKR was not statistically significant ($P = 0.172$). Similarly, with mobile C-arms, the difference in average AKR between adult and pediatric medical centers, as seen in Figure 4-4 and 4-5, was not found to be statistically significant ($P = 0.247$).

The reported data also demonstrate variability in the AKRs, pulse widths, and other collected parameters across the 131 units surveyed. These variations are partly due to the distribution in the age and design of the equipment surveyed. In addition, some differences are expected due to the relative performance requirements among clinical exams. For example, a mini C-arm and interventional fluoroscope are used for very different clinical procedures, and one expects the differences in design and performance to be substantial.

Due to its national overview and standardized protocol, TG-251 provides insight into the typical AKR values across different-sized simulated pediatric patients. QMPs can use the collected data to compare their measurements against typical values. For example, for a unit at the QMP's site, how does the AKR for a standard-size adult compare to the AKR reported here? If the results are similar, are the results also similar for the smallest and intermediate-sized patients? As a first approximation, the percent reductions for phantoms with thicknesses of 20, 15, 10, and 5 cm relative to the 25-cm phantom were 50%, 80%, 90%, and 95% (see Table 8). However, it is critical to keep in mind that the data reported cannot be used to establish DRLs. Any change in radiation dose settings must be accompanied by a thorough evaluation of clinical image quality (Strauss 2006b; Strauss 2015; Ubeda 2015).

4.2 Management/Configuration of Pediatric Interventional and Fluoroscopic Imaging Equipment

Because as many as 80% of pediatric patients are imaged at adult-oriented medical centers, QMPs, as part of a medical physics 3.0 initiative, should engage their manufacturers to obtain pediatric-specific exam protocols and configurations for each fluoroscope in their facility. High-quality images at appropriately managed patient doses for all patients from the 2-kg neonate to the 100-kg adult require configuration and radiographic technique changes, along with adjustments to image processing within the fluoroscope as patient size varies. The most effective configurations of fluoroscopic equipment for

pediatric imaging occur when the QMP and the manufacturer's representatives work together as a team, with the QMP identifying imaging objectives and manufacturer's rep identifying equipment adjustments available to address clinical needs. The process is complicated since adjustment to one parameter may require appropriate adjustments to a number of other parameters to maintain good image quality at properly managed radiation doses. A resource that QMPs can use to guide the configuration of protocols is the Medical Imaging and Technology Alliance (MITA) and Image Gently Alliance publication (MITA 2015), which outlines essential questions manufacturers should consider when designing interventional fluoroscopes intended for pediatric patients. An introduction to some of the important considerations and elements of this type of medical physics 3.0 initiative follows along with some references that provide more details.

State-of-the-art fluoroscopic systems provide many controls that can be accessed either in the service mode or clinical mode of operation to customize and match the performance of the fluoroscope to a specific diagnostic task (Miller 2010; Strauss 2006a & b). While equipment that uses factory default settings during pediatric examinations may produce satisfactory images, depending on the patient size, the patient dose may be greater than necessary, or the image quality may be less than optimal based on the machine's capabilities. In addition to frame rates and image receptor air kerma, many parameters under "Exam Protocols" or "Organ Programs" can be configured for each specific imaging task and saved for routine use. These parameters include, but are not limited to: focal spot size, added Cu filtration thickness, tube voltage, tube current, pulse width, and pulse rate. In addition, various post-processing options—such as noise reduction, edge enhancement, and default window and level settings—can be configured. Finally, proper configuration of the automatic dose rate control (ADRC) features introduced in section 4.4 is paramount to managing the patient's radiation dose. This allows users to maximize the strengths and minimize the weaknesses inherent in each manufacturer's fluoroscope designs.

4.3 Purchasing/Commissioning

During a new equipment selection process, hospitals and clinics should evaluate the vendor's ability to configure their unit to best utilize equipment features that address the unique imaging needs of the facility. Facilities should include a protocol configuration clause in their purchase contract that defines expectations and deliverables by the vendor during the installation and configuration of the equipment before its first clinical use. The contract should also define specific user expectations during the initial and follow-up applications training sessions. A clinical team—including a radiologist (or a cardiologist for cardiac procedures), a technologist, and a QMP—is necessary to work with the vendor's application specialists, product specialists, and field service engineers to discuss various aspects of the clinical configuration of the equipment (Strauss 2006b). Once optimized, protocols can be password protected, saved, modified, copied, and installed on compatible equipment throughout the institution. Suggested practices for managing imaging equipment from the initial identification of clinical requirements, equipment fluorographic planning, facility planning, construction, acceptance testing, staff education, equipment maintenance, and repair, to decommissioning, are discussed in detail elsewhere (Strauss 2006b).

It may not be realistic to design and optimize every protocol during the initial use of new equipment. Therefore, it is necessary to establish a manufacturer-customer partnership with the vendor whereby additional modifications and optimizations can be implemented as the site acclimates to the equipment or when new clinical procedures are implemented. One approach toward establishing partnerships is to have an upfront agreement during the purchase stages that allows end-users to manage, save, and back up protocols correctly.

4.4 Automatic Dose Rate Control Systems

In addition to the control parameters discussed previously, radiation doses delivered to the patient are dependent upon the configuration of the ADRC logic (AAPM 2012; Rauch 2012). The ADRC system monitors the AKR at the input surface of the detector. It modulates the x-ray tube output to deliver the target detector AKR during fluoroscopic or fluorographic imaging despite continual changes in the attenuation of the primary x-ray beam due to changes in patient anatomy or beam filtration. Modulation of the x-ray tube output also occurs when the distance between the detector entrance plane and focal spot changes (NCRP Report #168).

The appropriate target AKR at the detector is not only dependent on interpreting physician requirements (the acceptable level of noise in the fluoroscopic or fluorographic images), but also on the type of examination, the region of the body irradiated, and the size (or age) of the patient (Strauss 2015b). Once this baseline detector AKR is established for both fluoroscopy and fluorography, modulation of the base AKR should occur depending on the selected grid strategy as a function of patient size (Strauss 2015c), on the selected size of the field of view (Strauss 2006a), and on the pulse rate used during fluoroscopy (Aufrichtig 1994; Strauss 2006a).

While configurations described in this section have been demonstrated to effectively manage fluoroscopic and fluorographic image quality and patient dose during pediatric imaging in the clinical setting, the design constraints of different manufacturers' equipment may not permit all the described configuration changes. It is important to note that the Food and Drug Administration (FDA) does allow pediatric configurations to be applied to fluoroscopy devices (FDA 2017). The QMP should initiate and lead the process of exploring the feasibility and implementation of the suggested settings described above. This is an important aspect of Diagnostic Imaging Medical Physics 2.0 and 3.0 (Strauss 2014).

5. Conclusion

The charge of this task group was to collect AKR information as a function of phantom thickness to provide QMPs with baseline data to compare with their measured results. The reported data reflects the state of the practice across the United States and provides a standardized method for AKR measurement for various thicknesses of pediatric patient-equivalent materials. The methods and materials are feasible for consulting and for in-house QMPs to implement. Annual compliance testing of a fluoroscope must do more than measure the maximum AKR of a fluoroscope to establish that the fluoroscope is capable of reasonably managing the AKR during fluoroscopy for patients of all sizes, which may include small pediatric patients. A final key aspect of this report is that it describes a pathway for QMPs, regulatory bodies, and fluoroscope manufacturers to work together toward practical quality control methods that use phantom-based measurements to improve clinical practice.

6. References

American Association of Physicists in Medicine (AAPM). *Managing the Use of Fluoroscopy in Medical Institutions*. AAPM Report No. 58. Madison, WI: Medical Physics Publishing, 2012.

American Association of Physicists in Medicine (AAPM) (2018). "Position Statement on Radiation Risks from Medical Imaging Procedures." Accessed May 5, 2021: https://www.aapm.org/org/policies/details.asp?type=PP&id=439.

Aria, D., S. Vatsky, R. Towbin, C. M. Schaefer, and R. Kaye (2014). "Interventional radiology in the neonate and young infant." *Semin. Ultrasound CT MR* 35(6):588–607.

Aufrichtig, R., P. Xue, C. W. Thomas, G. C. Gilmore, and D. L. Wilson (1994). "Perceptual comparison of pulsed and continuous fluoroscopy." *Med. Phys.* 21(2):245–56.

Balter, S., B. A. Schueler, D. L. Miller, P. E. Cole, H. T. Lu, A. Berenstein, R. Albert, J. D. Georgia, P. T. Noonan, E. J. Russell, and T. W. Malisch (2004). "Radiation doses in interventional radiology procedures: The RAD-IR study: Part III: Dosimetric performance of the interventional fluoroscopy units." *J. Vasc. Interv. Radiol.* 15(9):919–26.

Balter, S. (2006). "Vendor question and answer panel." *Pediatr. Radiol.* 36(2):237–39.

Boone, J., et al. (1993). Task Group Report No. 11: Survey of fluoroscopic AKRs. *Med. Phys.* 29(3): 789–94.

Committee on Pediatric Emergency Medicine (CPEM) (2007). "Access to optimal emergency care for children." *Pediatrics* 119(1):161–64.

Damilakis, J. and A. Papadakis. *Radiation Dose Management of Pregnant Patients, Pregnant Staff and Paediatric Patients*. IOP Publishing Limited, 2019.

European Commission (EC) (2014). Radiation Protection No 180. "Diagnostic reference levels in thirty-six European countries." 2/2.

França, U. L. and M. L. McManus (2018). "Trends in regionalization of hospital care for common pediatric conditions." *Pediatrics* 141(1):e20171940.

Ferro, A. (2015). "Pediatric prescribing: why children are not small adults." *Br. J. Clin. Pharmacol.* 79(3):351–53.

Food and Drug Administration (FDA) (2017). Guidance for Industry and FDA Staff. Pediatric Information for X-Ray Imaging Device Premarket Notifications—Guidance for Industry and Food and Drug Administration Staff.

Hall, E. J. and A. J. Giaccia. *Radiobiology for the Radiologist*, 6th Ed. Lippincott Williams & Wilkins, 2006.

IGA (2014a). Image Gently®, https://www.imagegently.org/About-Us/The-Alliance (accessed July 19, 2018). Image Gently Alliance, Reston, Virginia.

IGA (2014b). Interventional Radiology—Step Lightly Resources. https://www.imagegently.org/Procedures/Interventional-Radiology/Image-Safely-Resources. Accessed July 19, 2018. Image Gently Alliance, Reston, Virginia.

IGA (2014c). Step Lightly Checklist. https://www.imagegently.org/Portals/6/Procedures/ImGen_StpLight_Chcklst.pdf. Accessed July 19, 2018. Image Gently Alliance, Reston, Virginia.

IGA (2014d). Steps for radiation safety in pediatric interventional radiology. https://www.imagegently.org/Portals/6/Procedures/Steps%20for%20Radiation%20Safety%20in%20Pediatric%20Interventional%20Radiology.pdf. Accessed July 19, 2018. Image Gently Alliance, Reston, Virginia.

International Commission on Radiological Protection (ICRP) (2007). ICRP publication 103. The 2007 Recommendations of the International Commission on Radiological Protection. *Ann ICRP* 37(2–4).

International Commission on Radiological Protection (ICRP) (2013). ICRP Publication 121. Radiological protection in paediatric diagnostic and interventional radiology. *Ann. ICRP* 42(2):1–66.

International Commission on Radiological Protection (ICRP) (2017). ICRP Publication 135. Diagnostic reference levels in medical imaging. *Ann. ICRP* 46(1):1–140.

International Commission on Radiation Units and Measurements (ICRU) (2005). Patient dosimetry for X-rays used in medical imaging. *J. ICRU* 5(2):1–19.

Kaye, R., S. S. Sane, and R. B. Towbin (2000). "Pediatric intervention: an update–part II. *J. Vasc. Interv. Radiol.* 11(7):807–22.

Kleinman, P. L., K. J. Strauss, D. Zurakowski, K. S. Buckley, and G. A.Taylor (2010). "Patient size measured on CT images as a function of age at a tertiary care children's hospital." *Am. J. Roentgenol.* 194(6):1611–19.

Kottou, S., N. Kollaros, C. Plemmenos, I. Mastorakou, S. C. Apostolopoulou, and V. Tsapaki (2018). "Towards the definition of Institutional diagnostic reference levels in paediatric interventional cardiology procedures in Greece." *Phys. Med.* 46:52–58.

Lederman, H. M., Z. P. Khademian, M. Felice, and P. J. Hurh (2002). "Dose reduction fluoroscopy in pediatrics." *Pediatr. Radiol.* 32(12):844–48.

Leyenaar, J. K., S. L. Ralston, M. S. Shieh, P. S. Pekow, R. Mangione-Smith, and P. K. Lindenauer (2016). "Epidemiology of pediatric hospitalizations at general hospitals and freestanding children's hospitals in the United States." *J. Hosp. Med.* 11(11):743–49.

Miller, D. L., S. Balter, B. A. Schueler, L. K. Wagner, K. J. Strauss, and E. Vano (2010). "Clinical radiation management for fluoroscopically guided interventional procedures." *Radiology* 257(2):321–32.

Medical Imaging and Technology Alliance and Image Gently Alliance (MITA) (2015). "Essential questions for consideration in the design of interventional x-ray equipment intended for pediatric use." https://www.medicalimaging.org/wp-content/uploads/2015/01/ Essential_Questions_to_design_Interventional_equipment_for_pediatric_18_Nov_2014.pdf.

NCRP. NCRP Report No. 168. *Radiation Dose Management for Fluoroscopically-Guided Interventional Medical Procedures*. Bethesda, MD: National Council on Radiation Protection and Measurements, 2010.

NCRP. NCRP Report No. 172. *Reference Levels and Achievable Doses in Medical and Dental Imaging: Recommendations for the United States*. Bethesda, MD: National Council on Radiation Protection and Measurements, 2012.

Rauch, P., P. J. P. Lin, S. Balter, A. Fukuda, A. Goode, G. Hartwell, T. LaFrance, E. Nickoloff, J. Shepard, and K. Strauss (2012). "Functionality and operation of fluoroscopic automatic brightness control/automatic dose rate control logic in modern cardiovascular and interventional angiography systems." A Report of Task Group 125 Radiography/Fluoroscopy Subcommittee, Imaging Physics Committee, Science Council. *Med. Phys.* 39(5):2826–28.

Ray, K. N., L. M. Olson, E. A. Edgerton, M. Ely, M. Gausche-Hill, P. Schmuhl, D. J. Wallace, and J. M. Kahn (2018). "Access to high pediatric-readiness emergency care in the United States." *J. Pediatr.* 194:225–32.

Sidhu, M. K., M. J. Goske, B. J. Coley, et al. (2009). "Image Gently, Step Lightly: Increasing radiation dose awareness in pediatric interventions through an international social marketing campaign." *J. Vasc. Interv. Radiol.* 20(9):1115–19.

Strauss, K. J. (2006a). "Pediatric interventional radiography equipment: Safety considerations." *Pediatr. Radiol.* 36(Suppl. 2):126–35.

Strauss, K.J. (2006b). "Interventional suite and equipment management: cradle to grave." *Pediatr. Radiol.* 36(Suppl. 2):221-236.

Strauss, K. J. (2014). "Fluoroscopy 2.0, Medical Physics 1.0 to 2.0, Session 2: Radiography, Mammography, and Fluoroscopy." *Med. Phys.* 41(6):491.

Strauss, K. J., J. M. Racadio, N. Johnson, et al. (2015a). "Estimates of diagnostic reference levels for pediatric peripheral and abdominal fluoroscopically guided procedures." *AJR Am. J. Roentgenol.* 204:W713–19.

Strauss, K. J., D. P. Frush, and M. J. Goske (2015b). "Image gently campaign: making a world of difference." *Med. Phys. Int.* 3(2):94–108.

Strauss, K. J., J. M. Racadio, T. A. Abruzzo, et al. (2015c). "Comparison of pediatric radiation dose and vessel visibility on angiographic systems using piglets as a surrogate: antiscatter grid removal vs. lower detector air kerma settings with a grid—a preclinical investigation." *JACMP* 16(5):408–17.

Strauss, K. J. (2019). "Advancing safety: Role of equipment design and configuration change in pediatric fluoroscopy." *Health Phys.* 116(2):256–62.

Sullivan, A. F., S. A. Rudders, A. L. Gonsalves, A. P. Steptoe, J. A. Espinola, and C. A. Camargo (2013). "National survey of pediatric services available in US emergency departments." *Int. J. Emerg. Med.* 6(1):1–6.

Ubeda, C., P. Miranda, and E. Vano (2015). "Local patient dose diagnostic reference levels in pediatric interventional cardiology in Chile using age bands and patient weight values." *Med. Phys.* 42:615–22.

Wagner, L. K., B. R. Archer, and A. M. Cohen (2000). "Management of patient skin dose in fluoroscopically guided interventional procedures." *J. Vasc. Interv. Radiol.* 11(1):25–33.

Wunderle, K. A., A. R. Godley, Z. L. Shen, J. T. Rakowski, and F. F. Dong (2017). "Percent depth doses and x-ray beam characterizations of a fluoroscopic system incorporating copper filtration." *Med. Phys.* 44(4):1275–86.

UNSCEAR (2013). "Sources, Effects and Risks of Ionizing Radiation." UNSCEAR 2013 Report, Volume II, Scientific Annex B: Effects of radiation exposure of children. New York: United Nations. http://www.unscear.org/docs/publications/2013/UNSCEAR_2013_Report_Vol.II.pdf.

Conflict of Interest Statement

The members of TG-251 listed below attest that they have no potential conflicts of interest related to the subject matter or materials presented in this document.

Usman Mahmood
Lawrence T. Dauer
Ishtiaq H. Bercha
Samuel L. Brady
Thomas M. Cummings
Cristina T. Dodge
David W. Jordan
Nima Kasraie
Mary A. Keenan
Mohammed H. Aljallad
Don-Soo Kim
Sarah E. McKenney
Richard Miguel
Donald L. Miller
Vikas Patel
David Spellic
Charles E. Willis
Xiaowei Zhu
Keith J. Strauss

The member of TG-251 listed below discloses the following potential conflict(s) of interest related to subject matter or materials presented in this document.

Andrew Kuhls-Gilcrist was employed by Cannon Medical, a commercial company, during the preparation of this report. This company played no role in the design, sponsorship, data collection, analysis, or preparation of the report and the decision to pursue publication.

APPENDIX

Abbreviations and Definitions Used in This Report

Con	continuous
EP	electrophysiology (i.e., IRC)
FPD	flat panel detector
II	image intensifier
IRR	interventional radiology
IRC	interventional cardiology unit
mGy/p	milli-gray per pulse
QMP	qualified medical physicist
SCD	source-to-chamber-surface distance
SID	source-to-image-receptor distance
SSD	source-to-skin distance
Std	standard
Var	variable